Regionally-selective cell colonization of micropatterned surfaces prepared by plasma polymerisation of acrylic acid and 1,7- octadiene

E. Filová[1,2,*], N.A. Bullett[3,4] L. Bačáková[1,2], Ľ. Grausová[1], J.W. Haycock[3], J. Hlučilová[5], J. Klíma[5,6], A. Shard[3,7]

[1]Department of Growth and Differentiation of Cell Populations and [2]Centre for Cardiovascular Research, Institute of Physiology v.v.i., Academy of Sciences of the Czech Republic, Videnska 1083, 142 20 Prague 4- Krc, Czech Republic, E-mail: filova@biomed.cas.cz

[3]Department of Engineering Materials, University of Sheffield, Sir Robert Hadfield Building, Mappin Street, Sheffield, UK S1 3JD

[4]Current Address: CellTran Ltd., The Innovation Centre, 217 Portobello, Sheffield, UK S1 4DP

[5]Institute of Animal Physiology and Genetics, v.v.i., Academy of Sciences of the Czech Republic, Rumburská 89, 277 21 Liběchov, Czech Republic

[6]Center of Cell Therapy and Tissue Repair, 2nd Faculty of Medicine, Charles University, U Nemocnice 3, 128 00 Prague 2, Czech Republic

[7]Current Address: National Physical Laboratory, Hampton Road, Middlesex, UK TW11 0LW

***Address for correspondence:**

Elena Filová, MSc.
Department of Growth and Differentiation of Cell Populations
Institute of Physiology v.v.i.
Academy of Sciences of the Czech Republic
Videnska 1083, 142 20 Prague 4- Krc
Czech Republic
Phone: +420 2 9644 2521, Fax: +420 2 9644 2488, +420 2 4106 2488, E-mail: filova@biomed.cas.cz

Short title: **Regionally-selective cell colonization of micropatterned surfaces**

Summary

Micropatterned surfaces have been used as a tool for controlling the extent and strength of cell adhesion, the direction of cell growth and the spatial distribution of cells. In this study, chemically micropatterned surfaces were prepared by successive plasma polymerisation of acrylic acid (AA) and 1,7-octadiene (OD) through a mask. Vascular smooth muscle cells (VSMC), endothelial cells (EC), mesenchymal stem cells (MSC) or skeletal muscle cells (HSKMC) were seeded on these surfaces in densities from 9,320 cells/cm^2 to 31,060 cells/cm^2. All cell types adhered and grew preferentially on the strip-like AA domains. Between day 1 and 7 after seeding, the percentage of cells on AA domains ranged from 84.5 to 63.3% for VSMC, 85.3 to 73.5% for EC, 98.0 to 90.0% for MCS, and 93.6 to 55.0% for HSKMC. The enzyme-linked immunosorbent assay (ELISA) revealed that the concentration of alpha-actin per mg of protein was significantly higher in VSMC on AA. Similarly, immunofluorescence staining of von Willebrand factor showed more apparent Weibel-Palade bodies in EC on AA domains. MSC growing on AA had better developed beta-actin cytoskeleton, although they were less stained for hyaluronan receptor (CD44). In accordance with this, MSC on AA contained a higher concentration of beta-actin, although the concentration of CD44 was lower. HSKMC growing on AA had a better developed alpha-actin cytoskeleton. These results based on four cell types suggest that plasma polymerisation is a suitable method for producing spatially defined patterned surfaces for controlled cell adhesion, proliferation and maturation.

Key words: micropatterning, plasma polymerisation, mesenchymal stem cells, endothelial cells, smooth muscle cells.

Introduction

One of the challenges in tissue engineering is to prepare materials for controlled cell attachment, growth, and migration. Cell attachment and adhesion to the surface of biomaterials are influenced by several factors, such as chemical composition, roughness, rigidity, wettability, surface energy, electrical charge, or protein adsorption (Bacakova *et al*. 2004). Abrupt transitions in physical-chemical properties have been successfully utilised to create discrete adhesive or non-adhesive domains for cells on micropatterned surfaces. The size and shape of the domains, and their periodicity, regulate the response of different cell types to the surface (Goessl *et al.* 2001).

Plasma polymerisation is a low-temperature, solvent-free process for the deposition of thin polymeric films from small volatile organic compounds (Alexander and Duck 1998, Kettle *et al.* 1997). Plasma discharge causes fragmentation of the monomer employed, creating a number of chemical functional groups, and crosslinking of the fragments. This crosslinking increases the stability of the polymer, and the content of ester groups, but decreases its solubility in water. This is accompanied by a decrease in functionality, mainly the–COOH group content that is thought to be essential for cell adhesion on copolymers of acrylic acid (AA) and 1,7-octadiene (OD). Monomer fragmentation can be reduced by precise regulation of the deposition parameters, mainly by plasma power and monomer flow rate. AA/OD copolymers prepared by plasma polymerisation have already been applied to direct adhesion of keratinocytes (Haddow *et al*. 1999, 2003) and ROS 17/2.8 osteoblast-like cells (Daw *et al*. 1998).

Synthetic polymers commonly used for constructing tissue replacements are often hydrophobic and do not allow satisfactory adhesion of cells. Patterned AA/OD copolymers with hydrophilic domains could optimise the cell delivery on the surface of a synthetic biomaterial in tissue engineering.

In this study we evaluated the adhesion and growth of vascular smooth muscle cells (VSMC), vascular endothelial cells (EC), mesenchymal stem cells (MSC) or skeletal muscle cells (HSKMC) on strip-like micropatterned surfaces created by plasma polymerisation of the monomers mentioned above, i.e. hydrophilic AA and hydrophobic OD. We observed preferential adhesion and growth of these four cell types on domains composed of acrylic acid. In addition, the maturation of cells, estimated by the concentration and arrangement of alpha-actin, beta-actin or von Willebrand factor, was usually higher on AA domains.

Materials and Methods

Plasma polymerisation

AA and OD were polymerised on the inner surface of 24-well multidishes (Costar, Falcon, Becton Dickinson, Lincoln Park, NJ) for cell culture experiments, and on Si wafers for XPS. The Si wafers were sonicated twice for 15 min each time with dichloromethane in ultrasound, once with methanol (Sigma Aldrich, UK) and dried with N_2. For plasma polymerisation, a glass cylindrical tube of internal diameter 10 cm and length 40 cm was used (QVF, UK). A copper coil was wound around the tube and earthed aluminium/brass flanges ended the tube connecting it with a radio frequency (RF) signal generator (Coaxial Power Systems Ltd., UK). The base pressure achieved was lower than 0.1×10^{-3} mBar and an operating pressure of 6.0×10^{-3} and 8.0×10^{-3} mBar was employed for acrylic acid and 1,7-octadiene, respectively. The leak rate was less than 0.01 $cm^3_{stp}min^{-1}$. The monomer for polymerisation was placed in round-bottomed flasks, connected to the reactor vessel via needle valves through one of the flanges. We used flow rate 2 $cm^3_{stp}min^{-1}$ and time of exposure 15 min and 1 min for AA and OD polymerisation, respectively. Plasma deposition for 15 min was used for preparing control surfaces composed of AA or OD without microdomains (referred to as C_AA or C_OD, respectively). The plasma was initiated and

sustained by a radiofrequency (RF) power source of frequency 13.56 MHz. Discharge powers of 5W and 10W were used for AA and OD, respectively. Impedance matching was used to ensure that the reflected RF power was minimised. The copper coil electrode is generally referred to as inductive coupling as opposed to capacitative coupling which would be two parallel plate electrodes. However, it has been shown that in this system, a large proportion of the energy coupling is capacitative due to the fact that the end flanges are earthed and also act as an electrode (Haddow *et al*. 1999).

After polymerisation of the first polymer, AA, in the form of a continuous layer on the dish bottom, the OD was polymerised through a mask consisting of a copper transmission electron microscope grid (Sjostrand Copper 3.05 mm, Athene Grids UK), with strip-like gaps that were 75 and 150 μm in width and 67.5 or 135 μm apart. The AA strips occupied 47% of the resulting patterned surface.

X-ray photoelectron spectroscopy

X-ray photoelectron spectroscopy (XPS) analyses of the polymer surfaces polymerised on Si wafers were performed using a VG CLAM 2 (VG, UK) X-ray photoelectron spectrometer. XPS was employed in the constant analyser energy mode using non-monochromatic Mg Kα X-rays with 1253.6 eV energy. Widescan spectra over the binding energy range 0-1100 eV were acquired using a pass energy of 100eV from each sample. Detailed spectra of the C 1s core levels were taken using 20eV pass energy. The relative sensitivity factors were experimentally determined from standard polymers during a routine monthly XPS calibration procedure. Peak fitting of the C 1s core line was carried out using WinESCA software (Scienta, Uppsala, Sweden), using a linear background subtraction and mixed Gaussian – Lorentzian peak shapes. The chemical shifts for C 1s environments were taken from the literature (Briggs 1998).

Condensation of water droplets

The presence of the pattern on the surface was confirmed by visualization of microscopic droplets of water condensed on to the material surface. Pictures of the patterned surface were taken immediately after wetting the surface by exposure of the sample to a humid atmosphere (phase-contrast microscope, Olympus IX 50, Japan).

Adsorption of collagen on to the surface

A solution of collagen IV conjugated with Oregon Green 488 (Molecular Probes, Eugene, OR, U.S.A.) was diluted in phosphate-buffered saline (PBS) to a concentration of 1 μg/ml. The collagen solution (0.5 ml) was poured into wells with polymerised surfaces and incubated for 24 hours at 4^{o}C, washed three times with PBS and digital images were captured under an epifluorescence microscope (Olympus IX50, digital camera DP70, Japan).

Contact angle measurement

The advancing water contact angles were measured on plasma polymer coated coverslips using the sessile drop method. A 2 μl drop of distilled water was placed on the surface, and the angles of the tangents to the points of contact were measured using a goniometer (Ramë-Hart, NJ, U.S.A.). Two further drops were added, and the contact angle was measured after each addition. For each surface, two separate points were analysed on three different surfaces.

Cells and culture conditions

VSMC were derived from the intima-media complex of the thoracic aorta of eight-week-old male Wistar SPF rats by the explantation method (Bacakova and Kunes 1995), and used in passage 4. The endothelial cells (EC) originated from bovine pulmonary artery (line CPAE

ATCC CCL-209, Rockville, MA, U.S.A.). Both cell types were seeded at a concentration of 31,060 cells/cm^2 in 1.5 ml of the following media: for VSMC, Dulbecco's Modified Eagle's Medium (Sigma, St. Louis, MO, U.S.A.; Cat No. D5648), supplemented with 10% of foetal bovine serum (FBS; Sebak GmbH, Aidenbach, Germany) and 40μg/ml of gentamicin (LEK, Ljubljana, Slovenia) was used, and the endothelial cells were grown in Minimum Essential Eagle Medium with 2mM L-glutamin, Earle`s BSS with 1.5 g/l sodium bicarbonate, 0.1 mM non-essential amino acids, 1.0 mM sodium pyruvate (all chemicals from Sigma) and 20% of FBS. EC did not adhere completely; therefore the medium was replaced in EC cultures 24 hours after seeding in order to remove the non-adherent cells.

Mesenchymal stem cells (MSC) were derived from a pig using the following procedure. Bone marrow blood was aspirated from os illium (*tuber coxae, ala ossis illii*) into a 10 ml syringe with 4 ml Dulbecco´s Phosphate Buffered Saline (PBS) with 2 % Fetal Bovine Serum (FBS, StemCell Technologies) and 5 IU heparin/mL connected with a hypodermic needle (20G/40 mm). The bone marrow blood (about 20 ml) was deposited over 15 ml of Ficoll-Paque PLUS (StemCell Technologies). After centrifugation at 400g for 30 min at room temperature, the dense gradient resulted in separation of erythrocytes and granulocytes as a pellet in the bottom part of the tube, while mononuclear cells were situated (located) in an opalescent layer between the lower Ficoll and the upper blood plasma. This layer was taken out, washed in a culture medium (see below) and used for propagation under *in vitro* conditions. Cells were seeded in tissue culture flasks at a density of approximately 5×10^5 cells/cm^2 and cultured at 37 ˚C in a humidified atmosphere with 5% of CO_2. The culture medium was an α-MEM medium (GIBCO) supplemented with 10% FBS (Sigma) and gentamycin (50 mg/ml, Sigma). After 24h of culture, the non-adherent cells were removed, and during subsequent cultivation (3 weeks), the medium was exchanged every third day. MSC were seeded in a density of 9320 cells/cm^2 in 1.5ml of α-MEM (GIBCO) medium

supplemented with 10% foetal bovine serum (FBS; Sebak GmbH, Aidenbach, Germany) and 40 μg/ml of gentamicin (LEK, Ljubljana, Slovenia). The presence of surface markers characteristic for MSC was then evaluated using flow cytometry. From passage 1 to 5, the cells were homogeneously stained for mesenchymal stem cell markers CD29, CD44 and CD90. At the same time, the cells were negative for CD45, i.e. a marker of leukocytes. Cells were also positively stained for markers CD105 and CD147 but the signal tended to decrease in subsequent passages. The concentration and spatial distribution of the hyaluronan receptor CD 44, i.e., an adhesion molecule which might influence the cell-material interaction, was then chosen as a marker of the further behavior of MSC on AA/OD patterned surfaces.

Human skeletal muscle cells (HSKMC) were represented by commercially available primary cultures isolated from human tissues at Provitro GmbH, Berlin, Germany. The cells were seeded in a density of 18,640 cells/cm^2 in 1.5 ml of skeletal muscle cell growth medium (Provitro GmbH, Germany; Cat. No. 201 0602) and used in passages 2 to 4.

Flow cytometry of mesenchymal stem cells

Trypsinized cells were washed in a blocking solution containing PBS supplemented with 10% FBS, 1% gelatin and 0,1% sodium azide. 5 x 10^5 cells were incubated in 100 μL of the blocking solution and 1 microgram of primary mAb for 30 minutes at 4°C. The panel of antibodies used was: anti-CD29 (clone MEM-101A), anti-CD105 (clone MEM 229), anti-CD147 (clone MEM-M6/2; all three antibodies from Exbio Praha a.s., Prague, Czech Republic), anti-CD44 (clone IM7), anti-CD90 (clone 5E10; both antibodies from BD Biosciences, San Jose, CA USA), anti-CD45 (clone K252-1E4, AbD Serotec, Kidlington, UK). After two washes in a washing solution (PBS with 1% gelatin and 0,1% azide), the cells were incubated with a goat anti-mouse Alexa Fluor 488 secondary antibody (Molecular Probes) in the blocking solution mentioned above (dilution 1:1000) for 30 min at 4°C.

Secondary antibody was washed out twice in the washing solution, and cell pellets were resuspended in the washing solution containing propidium iodide for determination of supravitality of the cells. Cells were then analysed by FACScalibur, and the data was processed using CellQuest software (BD Biosciences). CD44 staining was performed with PE conjugated primary antibody using similar conditions and buffers as mentioned above; isotype controls were included and served as background controls.

Cell number, morphology and growth curves

The number and shape of cells on the tested surfaces were evaluated on 9-15 micrographs taken under a phase-contrast microscope (Olympus IX50, Japan) equipped with a digital camera DP70. The cell population densities, measured from six hours to seven days after seeding were used for constructing the growth curves.

Bromodeoxyuridine labeling index

Three days after seeding, the cells were incubated with 40 μM 5-bromo-2-deoxy-uridine (BrdU; 30 min, 37^{o}C), washed with PBS, fixed with pre-cooled (-20°C) 70% ethanol for 15 min and their DNA was partially denatured by treatment with 3M HCl (20 min, room temperature). The samples were then washed in 0.1 M sodium tetraborate (pH 8.5, 10 min) and non-specific binding sites were blocked by 3% FBS in PBS with 0.3% Triton X-100 (Sigma, St. Louis, MO, U.S.A.) for 30 min. The newly synthesised DNA was immunolabelled with an anti-BrdU mouse monoclonal antibody (Exbio a.s. Praha, Vestec, CR, Cat. No. 11-286_M001; dilution 1:200) for 80 min at room temperature. Biotin-conjugated goat anti-mouse IgG (Fab specific, Sigma, St. Louis, MO, U.S.A., Cat. No. B-0529; dilution 1:300) and ExtrAvidin®-Peroxidase (Sigma, St. Louis, MO, U.S.A., Cat. No. E-2886; dilution 1:100) were used in the consequent steps. All three chemicals were diluted in PBS with 3% FBS and

0.3% Triton X-100 and applied for 60 min at room temperature. Then the solution containing a chromogen, 3, 3'- diaminobenzidine (1 mg), TRIS buffer (2 ml), and a peroxidase substrate, 1% peroxide (0.07 ml) was added. The colour was intensified by 8% $NiCl_2$ in H_2O for 5 min. The cells were counterstained with 0.5% light green and the percentage of BrdU-labelled nuclei was assessed in a phase-contrast microscope. For each experimental group, 11-15 randomly chosen microscopic fields were evaluated (0.138 mm^2, obj. 20x, 13-66 cells per field).

Immunofluorescence staining of alpha-actin, von Willebrand factor, beta-actin, CD44 and talin

Maturation of VSMC and EC was studied using immunofluorescence staining of markers of differentiation, such as alpha-actin and von Willebrand factor for VSMC and EC, respectively. Mesenchymal stem cells were stained for beta-actin, CD44 and talin, skeletal muscle cells for alpha- and beta-actin. The cells were fixed in 70% cold methanol (5 min, -20^{o}C), pre-treated with 3% FBS in PBS containing 0.1% Triton X-100 (20 min at room temperature) and incubated with primary antibodies, i.e. monoclonal anti-alpha smooth muscle actin (mouse IgG2a isotype, clone 1A4, Sigma, St. Louis, MO, U.S.A., Cat. No. A2547, dilution 1:200), rabbit anti-human von Willebrand factor (Sigma, Cat. No. F3520; dilution 1:100), monoclonal anti-beta-actin, clone AC-15, mouse ascites fluid (Sigma, Cat. No. A 5441; dilution 1:200), purified rat anti-pig CD44H (BD Biosciences, Cat. No. 551542; dilution 1:200) or monoclonal anti-talin (clone 8D4, Sigma St. Louis, MO, U.S.A.; Cat. No. T3287, dilution 1:200). All antibodies were diluted in PBS and applied for 80 min. As secondary antibodies, we used goat anti-mouse IgG fluorescein isothiocyanate (FITC) conjugate (Sigma, Cat. No. F-8771; dilution 1:200), goat anti-rabbit IgG FITC conjugate (Sigma, Cat. No. F-1262, dilution 1:40), Alexa Fluor®488-conjugated (F(ab`)2 fragment of

goat anti-mouse IgG (H+L), or Alexa Fluor®488-conjugated goat anti-rat IgG (H+L) (Molecular Probes, Cat. No. A11017 or A11006, dilution 1:400 or 1:200), respectively. The secondary antibodies were applied for 1 h at room temperature. The cells were mounted in Gel/mount™ (Biomeda Corp., CA, U.S.A.) and evaluated under an epifluorescence microscope (Olympus IX50, digital camera DP70, Japan).

Enzyme-linked immunosorbent assay (ELISA)

The concentration of alpha-actin, beta-actin, von Willebrand factor, hyaluronan receptor (CD44) and talin in cell lysates (per mg of protein) were measured after three-day cultivation on continuous non-patterned C_AA and C_OD surfaces (Tab 1.) The cells were detached by trypsinization (trypsin-EDTA, Sigma, St. Louis, MO, U.S.A., Cat. No. T4174; 5 min, 37°C), resuspended in PBS, centrifuged, resuspended in PBS (10^6 cells/ml) and kept in a freezer at -70°C overnight. The cell homogenates were then prepared by ultrasonication for 10 seconds by a sonicator (Bandelin Sonoplus HD 3080, BANDELIN electronic GmbH & Co. KG, Germany), and the total protein content was measured using a modified method by Lowry (Bacakova *et al*. 2000). Aliquots of the cell homogenates corresponding to 1–50 μg of protein in 50 μl of water were adsorbed on 96-well microtiter plates (Maxisorp, NUNC, Roskilde, Denmark) at 4°C overnight. After washing twice with PBS (100 μl/well), the non-specific binding sites were blocked by 0.02% gelatine in PBS (60 min, 100 μl/well). The primary monoclonal antibodies (see above), diluted in PBS, anti-alpha smooth muscle actin (dilution 1 : 250), monoclonal anti-beta-actin (dilution 1:200), anti-human von Willebrand factor (dilution 1: 200), or purified rat anti-pig CD44H (dilution 1:250) and monoclonal anti-talin (dilution 1:200) were applied for 60 min at room temperature (50 μl/well). As secondary antibodies, goat anti-mouse $F(ab')_2$ IgG fragment, goat anti-rabbit IgG (Sigma, St. Louis, MO, U.S.A.; Cat. No. A3682 and A9169, dilution 1 : 1000 and 1 : 5000, respectively); or goat

anti-rat IgG polyclonal antibody conjugated with peroxidase (SEROTEC, UK, Cat. No. STAR72, dilution 1:500) were used (diluted in PBS, 50 µl/well, incubation 45 min,). This step was followed by double washing in PBS with Triton X-100 (0.1%) and orthophenylendiamine reaction (Sigma, St. Louis, MO, U.S.A.; concentration 2.76 mM) using 0.05% H_2O_2 in 0.1 M phosphate buffer (pH 6.0, dark place, 100 µl/well). The reaction was stopped after 10–30 min by 2M H_2SO_4 (50 µl/well) and the absorbance was measured at 492 nm by a Wallac VICTOR^2, 1420 Multilabel Counter (PerkinElmer^{TM} LifeSciences, Belgium).

Statistical analysis

Quantitative data was presented as mean ± SEM (Standard Error of Mean). Statistical analyses were performed using SigmaStat (Jandel Corporation, U.S.A.). Multiple comparison procedures were carried out by the ANOVA, Student-Newman-Keuls method, a parametric test that compares the effect of a single factor on the mean of two or more groups. The value $p \leq 0.05$ was considered significant.

Results

Concentration of chemical functional groups

Only two elements were detected by XPS, namely carbon and oxygen (8 at% O and 42 at% O for OD and AA respectively). The chemically shifted species observed in C 1s spectra can thus be readily interpreted as belonging to oxygen-containing functionalities. Surfaces prepared by polymerisation of OD (Fig 1A, B) contained 92% C-C/H groups, 7% C-O/R groups, and 1% C=O groups. Polymeric AA (Fig.1C, D) contained C-C/H (58%), C-COOH/R (11%), C-OH/R (13%), C=O (7%).

Condensation of water droplets and collagen IV adsorption

Water droplets condensed on the surface proved the presence of a micropatterned structure (Fig. 1E). As indicated by the intensity of the fluorescence, Oregon Green 488-

conjugated collagen IV was more adsorbed on to OD domains (OD_lines) than on to AA domains (AA_lines, Fig 1F).

Contact angle

The figure shows the results of contact angle measurements of the plasma polymer surfaces. The hydrocarbon (octadiene) surface was relatively hydrophobic, as expected, having an advancing contact angle of 75.7±0.6º, measured in the plateau region of the graph. The acrylic acid surface was more hydrophilic, with an advancing contact angle measured as 47.8±0.6º (Fig 1G).

Adhesion and growth of VSMC on micropatterned AA/OD surfaces

During the 1st day after seeding VSMC (Fig. 2A-B) adhered preferentially on the strip-like AA_lines created by plasma polymerisation. The cells were spindle-shaped and oriented along the strips. Although the AA strips occupied only about 47% of the total surface area, the percentage of cells adhered on these domains amounted to 84.5 ± 3.1% (Fig. 3A). The steepest rise of the growth curve of VSMC on AA_lines from day 1 to 2 showed the earliest onset of cell proliferation on these domains (Fig. 3B). Moreover, VSMC growing on AA_lines was most active in DNA synthesis, as indicated by the highest BrdU labelling index of 12.2 ±1.3% measured on day 3 after seeding, compared to significantly lower values of 6.5 ± 1.4% and 7.5 ± 1.07% on OD_lines and C_OD, respectively. As a result, the population densities of VSMC on AA_lines during 7-day cultivation were significantly higher than those on OD_lines (Fig.3B). The density of VSMC on AA_lines even exceeded the density on a pure C_AA surface up to day 3 after seeding. The differences in cell adhesion and growth on AA and OD were more apparent on AA and OD strips than on continuous AA and OD surfaces. OD did not entirely inhibit cell adhesion and growth, but the cells reached only

relatively low densities on it. From day 1 to 7 after seeding, the densities on OD_lines were about 4.3 times lower than the values on AA_lines, and the densities on C_OD were ~1.7 times lower than on the corresponding C_AA surfaces. In addition, by day five after seeding, 54% of VSMC growing on OD_lines detached from the surface and floated in the culture media. On the other hand, it was observed that cells could span adjacent OD lines in order to reach a neighbouring AA domain (Fig. 2C). As a result, the difference in cell population densities between AA and OD lines gradually decreases. On day 7 after seeding, the percentage of cells on AA_lines decreased to 63.3 ± 2.2%, although this difference still remained significant (Fig. 3C).

Adhesion and growth of EC on a micropatterned AA/OD surface

Similarly to VSMC, endothelial cells also adhered and grew preferably on AA_lines (Fig. 2D-F). Six and 24 hours after seeding, the percentage of cells on these domains was 85.3 ± 3.8 and 80.7 ± 2.5, respectively (Fig. 4A). On day 1, the cells were mostly elongated along the direction of AA_lines, and in the following days they acquired a cobblestone-like appearance. The growth curves revealed that from day 1 to 7 after seeding, the cell number increased apparently only on AA_lines, whereas on the other surfaces, the changes in the cell number were minimal (Fig. 4B). The BrdU labelling index of EC amounted to 31.5 ± 3.4% on AA_lines, and was significantly higher than that on all other surfaces where the values ranged from 6.9 ± 0.9% to 13.5 ± 1.5%. The highest population density of EC was observed on AA_lines, the lowest on OD_lines each day during 7-day cultivation (Fig. 4 A-C). The difference in cell densities on AA and OD strips was much more apparent than that between surfaces with a continuous layer of AA or OD. On AA_lines, the densities were ~4.5 times higher than on OD_lines, whereas on C_AA, the values were only ~1.6. On day 7 after seeding, the percentage of EC growing on AA_lines was 73.5 ± 1.8% (Fig. 4C).

Adhesion and growth of MSC on a micropatterned AA/OD surface

Mesenchymal stem cells showed the most apparent preferential adhesion and growth on AA_lines (Fig. 2G-I). Six and 24 hours after seeding, the percentages of MSC growing on AA domains reached even 98.0 ± 1.0 and 90.2 ± 3.8, respectively. The cells growing on AA_lines were relatively less spread, often rounded, and no cell elongation, observed in VSMC and EC, along the strips was present (Fig. 2G-I). The highest cell population density was observed on AA domains during 7-day cultivation, and it was significantly higher than that on OD_lines (14.3 and 8.6 times higher on day 1 and 7 after seeding, respectively), as well as on both control non-patterned C_AA and C_OD samples (Fig. 5A). The lowest cell population density was found on OD_lines on day 1. Although the growth of MSC was very slow, as apparent from the growth curves (Fig. 5B), cells on AA_lines incorporated BrdU significantly more (BrdU labeling index of 50.5 ± 6.6%) than on OD_lines, and C_OD (17.7 ± 7.1%, and 17.0 ± 4.7%, respectively). The number of cells also increased on C_AA (Fig. 5B, C) during 1-week-cultivation, while on OD_lines this number stagnated from day 1 to 7. Pure C_OD did not allow cell growth, as the cell number decreased from day 1 to 7 (Fig. 5B). On day 7, the percentage of MSC growing on AA_lines was 90.0 ± 1.4.

Adhesion and growth of HSKMC on a micropatterned AA/OD surface

Also the human skeletal muscle cells adhered and grew preferentially on AA domains. Six hours and one day after seeding, 84.6 ± 1.6 and 93.6 ± 2.0 % of HSKMC were attached to these domains, respectively. Up to day 2 after seeding, the highest cell population densities were found on AA_lines, (Fig. 6A, B). Also the DNA synthesis on day 3 after seeding was the highest on AA_lines where it reached 34.8 ± 5.1% of BrdU positive cells, compared to significantly lower values of 24.5 ± 6.4% on OD_lines, and 28.2 ± 6.0% and C_OD. However, growth curves showed that between days 5 to 7 after seeding, the HSKMC

proliferation was quickest on continuous non-patterned C_AA surfaces (Fig. 6B). As a result, the cells on C_AA reached the highest cell population density on day 7, which was significantly higher than the values on the other surfaces (Fig. 6B-C). Moreover, on C_AA surfaces, the cells were markedly better spread than on the other surfaces, although the cells were polygonal in shape on all tested surfaces (Fig. 7M-O). Surprisingly, on day 7, the cell densities on both AA_lines and OD_lines were almost equal, with only 55.0% of HSKMC growing on AA_lines.

Immunoflurescence staining of alpha-actin, von Willebrand factor, beta-actin, CD44, and talin

VSMC growing on all surfaces had a well-developed alpha-actin cytoskeleton. Cells growing on OD were more spread, and thus it was easier to observe actin filaments after staining (Fig. 7 A-C). In EC, Von Willebrand factor, stored in Weibel-Palade bodies, was stained more intensively in cells growing on AA compared to OD (Fig. 7 D-F i.e., both strips and continuous layers). On micropatterned surfaces, positively stained EC created strips correspond to AA_lines (Fig. 7 D).

Surprisingly, CD44 was more intensively stained in MSC growing on C_OD, with the brightest staining at the cell-cell contacts. The highest concentration of CD44 in the area of cell-cell contacts was apparent also on micropatterned surfaces, but usually not on the pure C_AA surfaces (Fig. 7 G-I). At the same time, the cells on C_OD displayed less developed talin-containing focal adhesion plaques (Fig. 7 J-L). Beta-actin cytoskeleton was better developed and organized into thick bundles in MSC cultured on pure AA than on OD (Fig. 7 M-O). In comparison with cells on OD surfaces, HSKMC on AA domains, and especially on continuous C_AA surfaces, contained stronger alpha-actin filaments organized in parallel

bundles (Fig. 7P-R). However, such a clear difference between the AA surface and the OD surface was not observed when the cells were stained for beta-actin (data not shown).

Concentration of alpha-actin, von Willebrand factor, beta-actin, CD44 and talin

As revealed by ELISA, the concentration (per mg of protein) of alpha-actin, a marker of differentiation of muscle-type cells, such as VSMC and HSKMC, was significantly higher in VSMC growing on C_AA than growing on C_OD. However, in HSKMC, the concentrations of alpha-actin in cells growing on C_AA and C_OD were similar. Also the concentration of von Willebrand factor, a marker of endothelial cell maturation, was similar in EC on C_AA and C_OD (Tab. 1). Interestingly, MSC growing on C_OD contained significantly more CD44 than cells growing on C_AA. At the same time, the concentration of beta-actin in MSC growing on C_OD was significantly lower than in MSC on C_AA. The concentrations of beta-actin in VSMC, EC and HSKMC, as well as talin in all cell types were similar in cells growing on both C_AA and C_OD surfaces.

Discussion

We created surfaces patterned with strip-like domains of acrylic acid (AA) and 1, 7-octadiene (OD) characterized with preferential adhesion and growth of vascular smooth muscle cells (VSMC), endothelial cells (EC), mesenchymal stem cells (MSC) and skeletal muscle cells (HSKMC) on AA domains. This preferential cell colonization was probably due to a higher content of oxygen-containing chemical functional groups on these domains (Bacakova *et al*. 2000, 2001). This content is negatively correlated with the fragmentation of the polymer during plasma treatment, followed by crosslinking of the fragments. The most important parameter for regulating the process of fragmentation is plasma power. The highest fragmentation was observed at plasma power higher than 20W (Alexander and Duck 1998,

1999). Thus, we used lower values of plasma power, 10 and 5 W, for OD and AA, respectively, in order to provide sufficient functionality and also stability of the polymer. XPS measurement of AA on our samples revealed the presence of more than 10% of -COO-R/H groups after AA polymerisation. The positive influence of -COOH groups on cell attachment on the surface composed of acrylic acid/1,7-OD copolymer was observed in a study on osteoblast-like cells (ROS17/2.8) and human keratinocytes. The best attachment was observed on surfaces with 3% and 2.3% of -COOH group on the surface layer, respectively (Daw *et al*. 1998, France *et al*. 1998). Similarly, in our earlier study performed on VSMC cultured on polylactide/poly(ethylene oxide)-based surfaces, we observed slightly improved adhesion and proliferation of VSMC on surfaces bearing -COOH (Bacakova *et al*. 2003). Also other oxygen-containing groups, such as -C=O, -C-O-H/R and -C-O-C-, produced during the plasma polymerisation process, could contribute to the improved adhesion of VSMC and EC to AA surfaces (Bacakova *et al*. 2000, 2001).

The presence of oxygen-containing groups on the biomaterial surface is usually associated with its increased wettability (Bacakova *et al*. 2000, 2001, 2003). In accordance with these findings, our AA surfaces were more hydrophilic than OD, although the contact angle of polymerised AA measured in the previous study was as low as 17º (Bullett *et al.* 2003). Highly hydrophilic surfaces are known for low or even absent adsorption of proteins from the culture media or body fluids, including cell adhesion-mediating extracellular matrix proteins, namely vitronectin, fibronectin, collagen and laminin. Our results confirmed that collagen IV, an important component of cellular basal lamina, was adsorbed preferably on hydrophobic OD regions. In another study, collagen was adsorbed in a higher amount on more hydrophobic polystyrene than on plasma-oxidized and more hydrophilic polymer (PSox). However, collagen layers adsorbed on PSox were smoother and showed higher mechanical stability (Pamuła *et al*. 2004). Improved mechanical properties together with an appropriate

spatial conformation of the adsorbed proteins could also contribute to the preferential cell adhesion on hydrophilic AA. Moreover, in our cell culture system, the selectivity of cell adhesion may be further enhanced by competitive adsorption of plasma proteins. It is known that albumin, which is non-adhesive for cells, is adsorbed preferentially to hydrophobic surfaces, whereas fibronectin, a cell adhesion-mediating protein, is adsorbed in an active conformation (i.e., accessible for cell adhesion receptors) only on hydrophilic surfaces (Dewez *et al*. 1999). Similarly, the amount of immunoglobulin G adsorbed onto COOH-functionalized surfaces was lower, but this protein was better accessible for antibodies (Bullett *et al*. 2003).

On the other hand, the addition of a small amount of albumin to a fibronectin solution improved fibronectin conformation on a hydrophobic surface (Grinnell and Feld 1982). This may explain our finding that hydrophobic OD surfaces were not completely antiadhesive for cells.

Goessl and co-workers (Goessl *et al*. 2001) revealed that VSMC needed a minimum area of 400 μm^2 for attachment and spreading, and larger areas were often occupied by more cells, which created cell agglomerates where individual cells were overlapped. It is in accordance with our results that VSMC grew in very high density on relatively wide AA strips with the area ranging from approx. 94,000 to 300,000 μm^2. EC derived from human tendon granuloma and cultivated on nanostructured poly(4-bromostyrene) increased and accelerated their spreading and changed their shape to arcuate or curved, which is considered to be more natural (Dalby *et al*. 2002). On our micropatterned samples, we observed more elongated morphology of EC, which is often observed in three-dimensional cultivating systems (Davis *et al*. 2002). In addition, this morphology is a sign of immature, proliferating endothelium, e.g. during angiogenesis (Davis *et al*. 2002). A certain immaturity of endothelial cells may explain our finding that the endothelial cells on AA surfaces were not able significantly to

increase their content of von Willebrand factor, which is a marker of differentiation of EC. Another cause may be the line origin of our EC, which could be associated with some irreversible loss of cell differentiation markers (Fisher and Tickle, 1981). On the other hand, immunofluorescence revealed that in cells on AA surfaces, von Willebrand factor was better organized into Weibel-Palade bodies. On AA, not only did we observe preferential adhesion of VSMC but this in turn led to an increase in protein synthesis of alpha-actin. The higher concentration of alpha-actin in VSMC seems to be an advantageous property for the maintenance of VSMC in differentiated contractile phenotype, which is necessary for their proper functions on artificial vessels.

Preferential cell colonization on hydrophilic AA domains was further enhanced by additional cell migration from adjacent hydrophobic regions. Both EC and VSMC are able to produce chemotactic and growth factors such as HB-EGF, bFGF, TGF-β1, PDGF-AA, and PDGF-BB, which regulate their migration, proliferation and phenotypic modulation (Raab and Klagsbrun 1997, Von Offenberg Sweeney *et al*. 2004).

Mesenchymal stem cells were most sensitive to the physical and chemical surface properties during the entire cultivation period, as indicated by the highest regional selectivity of their adhesion and growth on AA domains. This might be due to their relatively low maturation status and thus high responsiveness to extracellular signals controlling their growth and differentiation (Engler *et al.* 2006). Another possible cause might be that these cells proliferated very slowly, and thus they were not able to grow out of AA lines and span adjacent OD lines like VSMC. On continuous C_OD surfaces, MSC increased their synthesis of CD44, a receptor for hyaluronic acid. This could be explained as a compensatory mechanism to improve cell adhesion on a surface that is less convenient for cell adhesion, as indicated by less developed talin-containing focal adhesion plaques in MSC on C_OD. The preferential localization of CD44 at the regions of cell-cell contacts suggests that this

compensatory mechanism involves enhancement of cell-cell adhesion (Yang and Binns 1993). Activated CD44 receptor is known to induce actin polymerization (Bourguignon *et al.* 2007). However, in MSC on C_OD surfaces, the organization of beta-actin into cytoskeletal fibres and even its concentration was lower than in cells on C_AA surfaces.

Interestingly, on continuous non-patterned C_AA surfaces, skeletal muscle HSKMC cells reached an almost twice higher population density than on AA_strips on day 7 after seeding. This could be explained by the fact that continuous C_AA surfaces offered a larger area, more favourable for cell adhesion and growth than relatively narrow AA strips. In addition, the skeletal muscle cells are able to synthesize growth factors like IGF-1 and IGF-II (Semsarian *et al*. 1999). The concentrations of these factors in cultures on C_AA might be higher because the total number of HSKMC cells in these cultures was higher from the onset of cultivation. The enhanced growth of HSKMC cells on C_AA surfaces was accompanied by a more pronounced organization of alpha-actin molecules into thick filaments oriented in parallel. In muscle cells, organization of alpha-actin could be considered as a sign of maturation and acquisition of contractile phenotype. On the other hand, the concentration of alpha-actin in cells on C_AA was similar as on C_OD.

Micropatterned surfaces can be practically used in construction of tissue replacements and tissue engineering. For example, micro-textured polyurethane seeded with EC exposed to shear stress using a dynamic cultivation system was able to increase significantly (by 36%) the retention of EC compared to a non-patterned polyurethane surface (Daxini *et al*. 2006). This suggests that the patterned surfaces developed in this study might be used for constructing bioartificial vascular grafts, where it is highly desirable to coat the inner surface with a continuous endothelial cell layer. Another example is provided by the two- and three-dimensional micropatterned thermoresponsive surfaces used for co-culture of hepatocytes and endothelial cells for potential construction of bioartificial liver tissue [Hirose *et al*. 2000].

Conclusions

We have constructed micropatterned surfaces containing hydrophilic and hydrophobic strip-like domains prepared by plasma polymerization of acrylic acid (AA) and 1,7-octadiene (OD), respectively. Four cell types, represented by rat vascular smooth muscle cells (VSMC), bovine vascular endothelial cells (EC), porcine mesenchymal stem cells (MSC) and human skeletal muscle cells (HSKMC) preferentially recognized the hydrophilic AA domains for their adhesion and growth. However, these cell types differed in their responses, such as their shape, cytoskeletal organization, maturation and proteosynthesis. VSMC and EC were more elongated along AA strips, whereas the other cell types were round or polygonal. Actin cytoskeleton was better organized in MSC and HSKMC on AA. Cells on AA were usually more mature, as indicated by stronger staining for von Willebrand factor (EC), thick alpha-actin filaments (HSKMC) and a higher concentration of alpha-actin (VSMC). MSC on OD domains synthesized more CD44, a receptor for hyaluronic acid. Therefore, the patterned surfaces provide a control over spatial distribution as well as adhesion, growth and differentiation behavior of cell. Thus, they have significant potential for applications in tissue engineering, as information on the ability to influence cell distribution using surface chemical group deposition will be of value in developing 3-dimensional tissue constructs.

Acknowledgements

The study was supported by the Grant Agency of the Academy of Sciences of the Czech Republic (grant No. A 5011301). We also thank Mrs. Ivana Zajanová (Inst. Physiol., Acad. Sci. CR) for her excellent technical assistance and Mr. Robin Healey (Czech Technical University, Prague) for the language revision of the manuscript.

References

ALEXANDER MR, DUC TM: A study of the interaction of acrylic acid/1,7-octadiene plasma deposits in water and other solvents. *Polymer* **40**: 5479-5488, 1999.

ALEXANDER MR, DUCK TM: The chemistry of deposits formed from acrylic acid plasmas. *J Mat Chem* **8**: 937-943, 1998.

BACAKOVA L, FILOVA E, RYPACEK F, SVORCIK V, STARY V: Cell adhesion on artificial materials for tissue engineering. *Physiol Res* **53** (Suppl.1): 35-45, 2004.

BACAKOVA L, KUNES J: Sex-dependent differences in growth of vascular smooth muscles cells from spontaneously hypertensive rats. *Physiol Res* **44**: 127-130, 1995.

BACAKOVA L, LAPCIKOVA M, KUBIES D, RYPACEK F: Adhesion and growth of rat aortic smooth muscle cells on lactide-based polymers. *Adv Exp Med Biol* **534**: 179-189, 2003.

BACAKOVA L, MARES V, LISA V, SVORCIK V: Molecular mechanisms of improved adhesion and growth of an endothelial cell line cultured on polystyrene implanted with fluorine ions. *Biomaterials* **21**: 1173-1179, 2000.

BACAKOVA L, WALACHOVA K, SVORCIK V, HNATOWITZ V: Adhesion and proliferation of rat vascular smooth muscle cells (VSMC) on polyethylene implanted with O(+) and C(+) ions. *J Biomater Sci Polym Ed* **12**: 817-834, 2001.

BOURGUIGNON LY, PEYROLLIER K, GILAD E, BRIGHTMAN A: Hyaluronan-CD44 interaction with neural Wiskott-Aldrich syndrome protein (N-WASP) promotes actin polymerization and ErbB2 activation leading to beta-catenin nuclear translocation, transcriptional up-regulation, and cell migration in ovarian tumor cells. *J Biol Chem* **282**: 1265-1280, 2007.

BRIGGS D: Surface Analysis of Polymers by XPS and Static SIMS, Cambridge University Press, 1998, pp 65-66.

BULLETT NA, WHITTLE JD, SHORT RD, DOUGLAS CWI: Adsorption of immunoglobulin G to plasma-co-polymer surface of acrylic acid and 1,7-octadiene. *J Mater Chem* **13**: 1546-1553, 2003.

DALBY MJ, RIEHLE MO, JOHNSTONE H, AFFROSSMAN S, CURTIS AS: In vitro reaction of endothelial cells to polymer demixed nanotopography. *Biomaterials* **23**: 2945-2954, 2002.

DAVIS GE, BAYLESS KJ, MAVILA A: Molecular basis of endothelial cell morphogenesis in three-dimensional extracellular matrices. *Anat Rec* **268**: 252-275, 2002.

DAW R, CANDAN S, BECK AJ, DEVLIN AJ, BROOK IM, MACNEIL S, DAWSON RA, SHORT RD: Plasma copolymer surface of acrylic acid/1,7-octadiene: Surface characterisation and the attachment of ROS 17/2.8 osteoblast-like cells. *Biomaterials* **19**: 1717-1725, 1998.

DAXINI SC, NICHOL JW, SIEMINSKI AL, SMITH G., GOOCH KJ, SHASTRI VP: Micropatterned polymer surfaces improve retention of endothelial cells exposed to flow-induced shear stress. *Biorheology* **43**: 44-45, 2006.

DEWEZ JL, DOREN A, SCHNEIDER YJ, ROUXHET PG: Competitive adsorption of proteins: Key of the relationship between substratum surface properties and adhesion of epithelial cells. *Biomaterials* **20**: 547-559, 1999.

ENGLER AJ, SEN S, SWEENEY HL, DISCHER DE: Matrix elasticity directs stem cell lineage specification. *Cell* **126**: 677-689, 2006.

FISHER PE, TICKLE C: Differences in the alignment of normal and transformed cells on glass fibres. *Exp Cell Res* **131**: 407-409, 1981.

FRANCE RM, SHORT RD, DAWSON RA, MACNEIL S: Attachment of human keratinocytes to plasma co-polymers of acrylic acid/octa-1,7-diene and allyl amine/octa-1,7-diene. *J Mater Chem* **8**: 37-42, 1998.

GOESSL A, BOWEN-POPE DF, HOFFMAN AS: Control of shape and size of vascular smooth muscle cells *in vitro* by plasma lithography. *J Biomed Mater Res* **57**: 15-24, 2001.

GRINNELL F, FELD MK: Fibronectin adsorption on hydrophilic and hydrophobic surfaces detected by antibody binding and analyzed during cell adhesion in serum-containing medium. *J Biol Chem* **257**: 4888-4893, 1982.

HADDOW DB, FRANCE RM, SHORT RD, DAWSON RA, LEGGET GJ, COOPER E: Comparison of proliferation and growth of human keratinocytes on plasma copolymers of acrylic acid/1,7-octadiene and self-assembled monolayers. *J Biomed Mater Res* **47**: 379-387, 1999.

HADDOW DB, STEELE DA, SHORT RD, DAWSON RA, MACNEIL S: Plasma-polymerized surfaces for culture of human keratinocytes and transfer of cells to an *in vitro* wound-bed model. *J Biomed Mater Res* **64A**: 80-87, 2003.

HIROSE M, YAMATO M, KWON OH, HARIMOTO M, KUSHIDA A, SHIMIZU T, KIKUCHI A, OKANO T: Temperature-responsive surface for novel co-culture systems of hepatocytes with endothelial cells: 2-D patterned and double layered co-cultures. *Yonsei Med J*. **41:** 803-813, 2000.

KETTLE AP, BECK AJ, O'TOOLE L, JONES FR, SHORT RD: Plasma polymerisation for molecular engineering of carbon-fibre surfaces for optimised composites. *Comp Sci Technol* **57:** 1023-1032, 1997.

PAMUŁA E, DE CUPERE V, DUFRENE YF, ROUXHET PG: Nanoscale organization of adsorbed collagen: Influence of substrate hydrophobicity and adsorption time. *J Colloid Interface Sci* **271**: 80-91, 2004.

RAAB G**,** KLAGSBRUN M: HEPARIN-BINDING EGF-LIKE GROWTH FACTOR: *Biochim Biophys Acta* **1333**: F179-199, 1997.

SEMSARIAN C, SUTRAVE P, RICHMOND DR, GRAHAM RM: Insulin-like growth factor (IGF-I) induces myotube hypertrophy associated with an increase in anaerobic glycolysis in a clonal skeletal-muscle cell model. *Biochem J* **339**: 443-451, 1999.

VON OFFENBERG SWEENEY N, CUMMINS PM, BIRNEY YA, REDMOND EM, A. CAHILL PA: Cyclic strain-induced endothelial MMP-2: role in vascular smooth muscle cell migration. *Biochem Biophys Res Commun* **320**: 325-333, 2004.

YANG H, BINNS RM: CD44 is not directly involved in the binding of lymphocytes to cultured high endothelial cells from peripheral lymph nodes. *Immunology* **79**: 418-24, 1993.

Fig. 1. **A, B**: wide (A) and narrow (B) XPS spectrum of polymerised 1,7- octadiene; **C, D**: wide (C) and narrow (D) spectrum of polymerised acrylic acid; **E, F**: visualization of a micropatterned surface by condensation of water, objective 4x (E); adsorption of collagen IV, objective 20x (F); **G:** Advancing water contact angles on polymerised acrylic acid and 1,7-octadiene using the sessile drop method (G).

Fig. 2. Vascular smooth muscle cells (A-C), endothelial cells (D-F), mesenchymal stem cells (G-I) or skeletal muscle cells (J-L) on micropatterned surfaces with acrylic acid and 1,7-octadiene domains, 6 hours (A, D, G, J), 24 hours (B, E, H, K) and 5 days (C, F, I, L) after seeding. Lines in pictures (D-L) indicate AA strips on the patterned surface. Olympus IX50, digital camera DP70, obj.×20 (A and D) and ×10 (2B-C, E-L). Bar: A: 100 µm, B-L: 200 µm.

Fig. 3. Population density of vascular smooth muscle cells (VSMC) on strips formed by AA (*AA_lines*), OD (*OD_lines*), on control surface without microdomains formed by AA (*C_AA*) and OD (*C_OD*) on day 1 (**A**) and on day 7 after seeding (**C**). Growth curves (**B**) of VSMC cultivated on these surfaces. Mean ± SEM from 9 to 15 measurements, ANOVA; #, §, £, ∞: $p \leq 0.05$ in comparison with AA_lines, OD_lines, C_AA and C_OD, respectively.

Fig. 4. Population density of vascular endothelial cells (EC) on strips formed by AA (*AA_lines*), OD (*OD_lines*), on a control surface without microdomains formed by AA (*C_AA*) and OD (*C_OD*) on day 1 (**A**) and on day 7 after seeding (**C**). Growth curves (**B**) of EC cultivated on these surfaces. Mean ± SEM from 9 to 15 measurements, ANOVA; #, §, £, ∞: $p \leq 0.05$ in comparison with AA_lines, OD_lines, C_AA and C_OD, respectively.

Fig. 5. Population density of mesenchymal stem cells (MSC) on strips formed by AA (*AA_lines*), OD (*OD_lines*), on a control surface without microdomains formed by AA (*C_AA*) and OD (*C_OD*) on day 1 (**A**) and on day 7 after seeding (**C**). Growth curves (**B**) of MSC cultivated on these surfaces. Mean ± SEM from 10 to 12 measurements, ANOVA; #, §, £, ∞: p≤0.05 in comparison with AA_lines, OD_lines, C_AA and C_OD, respectively.

Fig. 6. Population density of human skeletal muscle cells (HSKMC) on strips formed by AA (*AA_lines*), OD (*OD_lines*), on a control surface without microdomains formed by AA (*C_AA*) and OD (*C_OD*) on day 1 (**A**) and on day 7 after seeding (**C**). Growth curves (**B**) of HSKMC cultivated on these surfaces. Mean ± SEM from 12 to 17 measurements, ANOVA; #, §, £, ∞: p≤0.05 in comparison with AA_lines, OD_lines, C_AA and C_OD, respectively.

Fig. 7. Immunofluorescence staining of alpha-actin in vascular smooth muscle cells (A-C); von Willebrand factor in endothelial cells (D-F), CD44 (G-I), talin (J-L) and beta-actin (M-O) in mesenchymal stem cells; and alpha-actin in skeletal muscle cells (P-R) growing on domains composed of acrylic acid (A, D, G, J, M, P), pure acrylic acid (B, E, H, K, N, Q), and pure 1,7-octadiene (C, F, I, L, O, R). Olympus IX50, digital camera DP70, obj.×20x, bar = 100 µm (A-F, J, M-P); obj.×10 (G), bar = 200 µm; and obj.×40, bar = 50 µm (H, I, K, L, Q, R).

Tab. 1. Enzyme-linked immunosorbent assay (ELISA) of alpha-actin, beta-actin, talin, von Willebrand factor or CD44 in vascular smooth muscle cells, endothelial cells, mesenchymal stem cells or skeletal muscle cells. The absorbance on C_OD was expressed as a percentage of the values obtained in cells on C_AA. Mean ± SEM from 3 to 8 measurements, ANOVA, *p≤ 0.05 compared to C_AA.

E L I S A					
C_AA	**C_OD** *(% C_AA)*	**C_AA**	**C_OD** *(% C_AA)*	**C_AA**	**C_OD** *(% C_AA)*
VSMC (alpha-actin)		**VSMC (beta-actin)**		**VSMC (talin)**	
100.0±4.2	77.1±9.2*	100.0±12.4	83.5±17.9	100.0±10.7	82.9±5.1
EC (von Willebrand factor)		**EC (beta-actin)**		**EC (talin)**	
100.0±3.5	92.0±6.9	100.0±9.95	123.4±22.8	100.0±6.0	97.9±2.9
MSC (CD44)		**MSC (beta-actin)**		**MSC (talin)**	
100.0±12.0	152.3±3.2*	100.0±6.97	75.2±7.8*	100.0±5.8	95.8±6.0
HSKMC (alpha-actin)		**HSKMC (beta-actin)**		**HSKMC (talin)**	
100.0±10.0	95.8±7.5	100.0±12.9	114.1±16.7	100.0±5.8	110.9±8.5

Fig. 1.

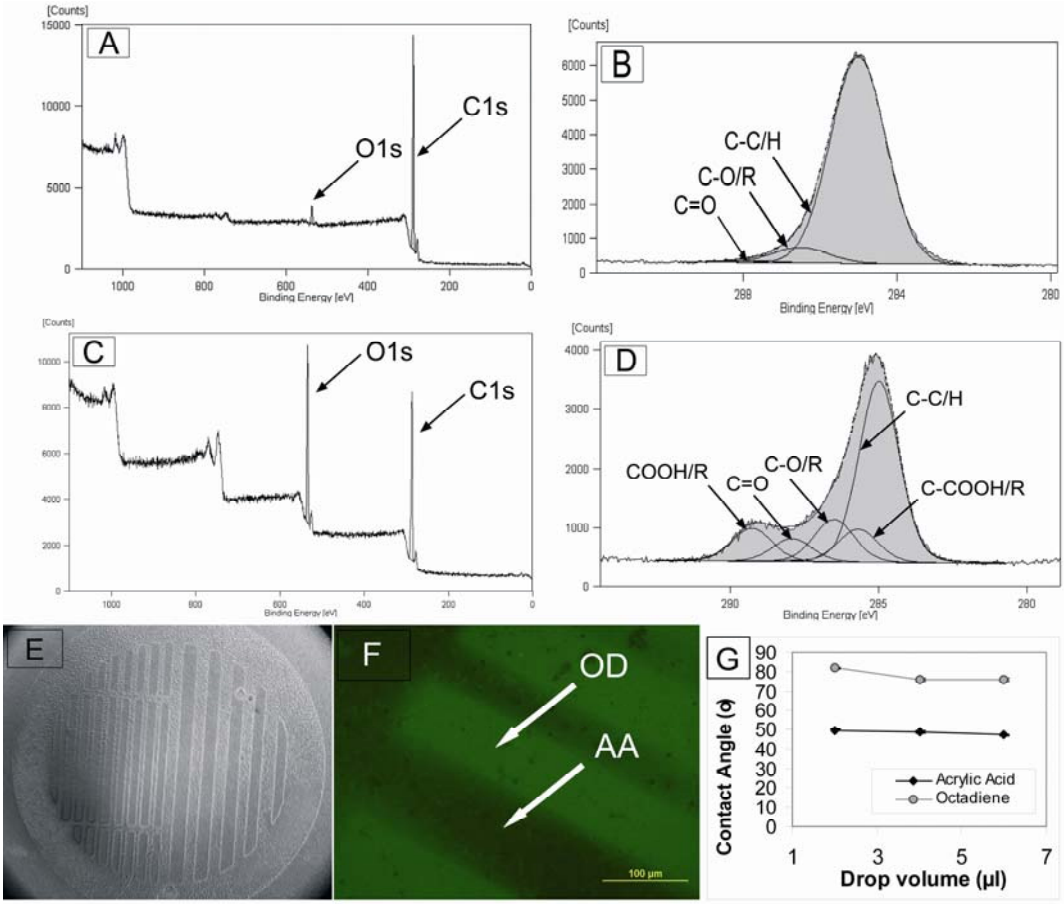
A
[Counts]
15000
10000
5000
0
O1s
C1s
1000
800
600
400
200
0
Binding Energy [eV]
B
[Counts]
6000
5000
4000
3000
2000
1000
0
C-C/H
C-O/R
C=O
288
284
280
Binding Energy [eV]
C
[Counts]
O1s
C1s
Binding Energy [eV]
D
[Counts]
4000
3000
2000
1000
0
C-C/H
COOH/R
C=O
C-O/R
C-COOH/R
290
285
280
Binding Energy [eV]
E
F
OD
AA
100 µm
G
Contact Angle (ϕ)
90
80
70
60
50
40
30
20
10
0
Acrylic Acid
Octadiene
1
3
5
7
Drop volume (µl)

Fig. 2.

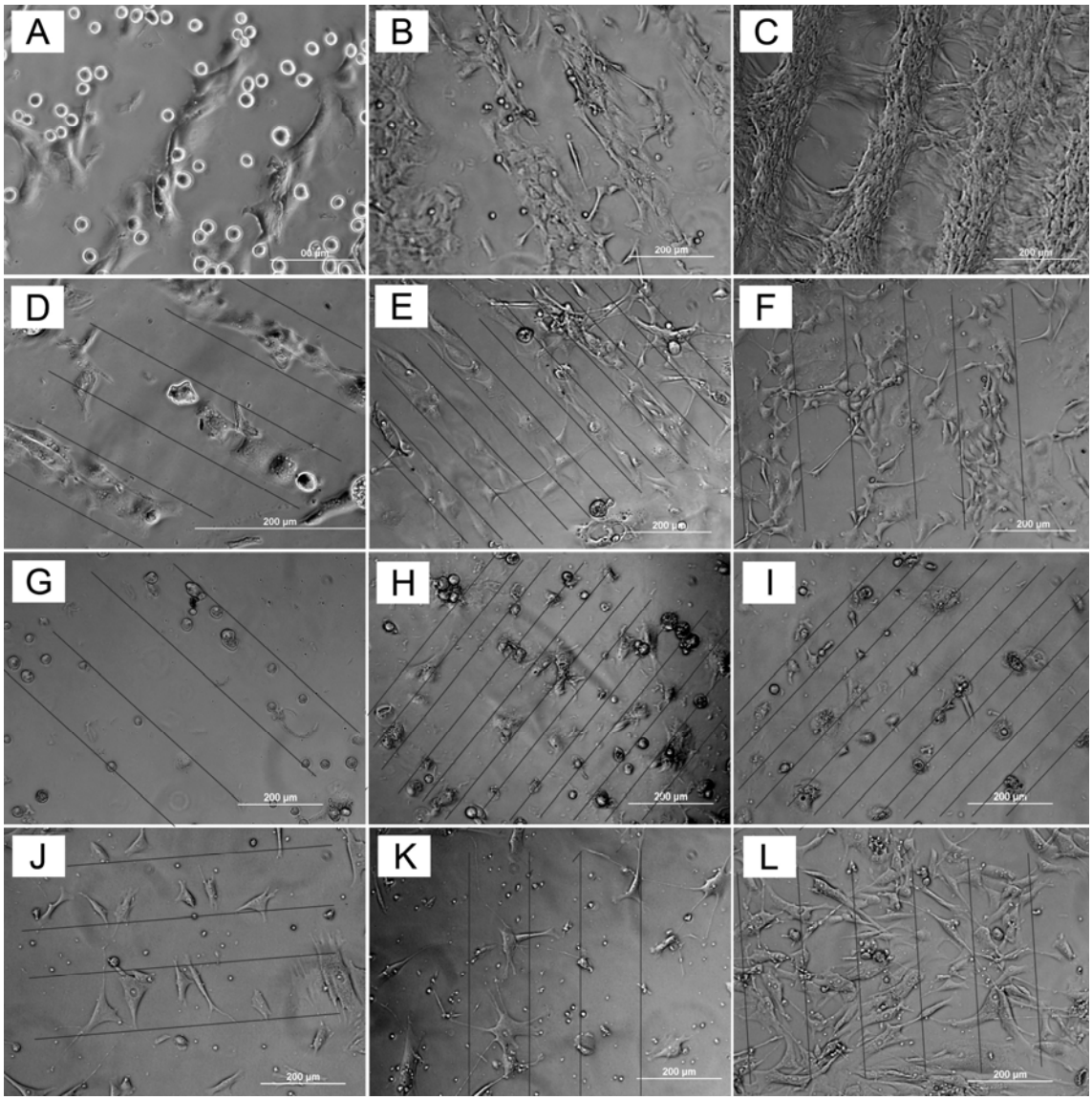

Fig. 3.

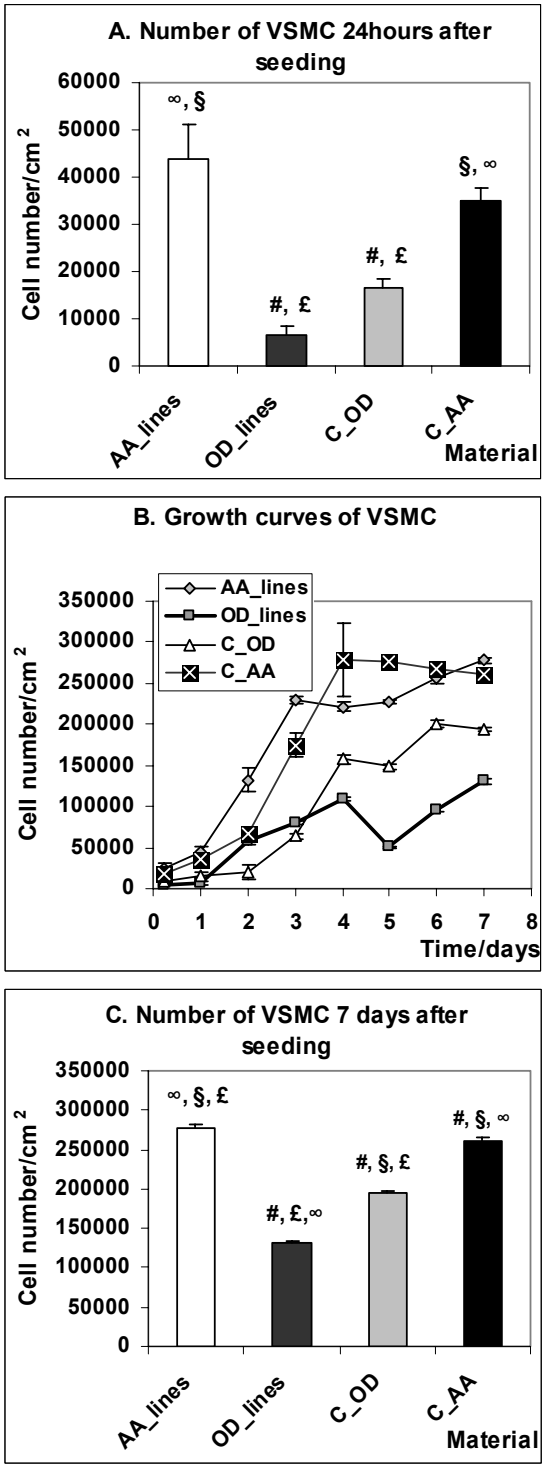
A. Number of VSMC 24hours after seeding
Cell number/cm 2
60000
50000
40000
30000
20000
10000
0
∞, §
#, £
#, £
§, ∞
AA_lines
OD_lines
C_OD
C_AA
Material
B. Growth curves of VSMC
Cell number/cm 2
350000
300000
250000
200000
150000
100000
50000
0
AA_lines
OD_lines
C_OD
C_AA
0 1 2 3 4 5 6 7 8
Time/days
C. Number of VSMC 7 days after seeding
Cell number/cm 2
350000
300000
250000
200000
150000
100000
50000
0
∞, §, £
#, £,∞
#, §, £
#, §, ∞
AA_lines
OD_lines
C_OD
C_AA
Material

Fig. 4.

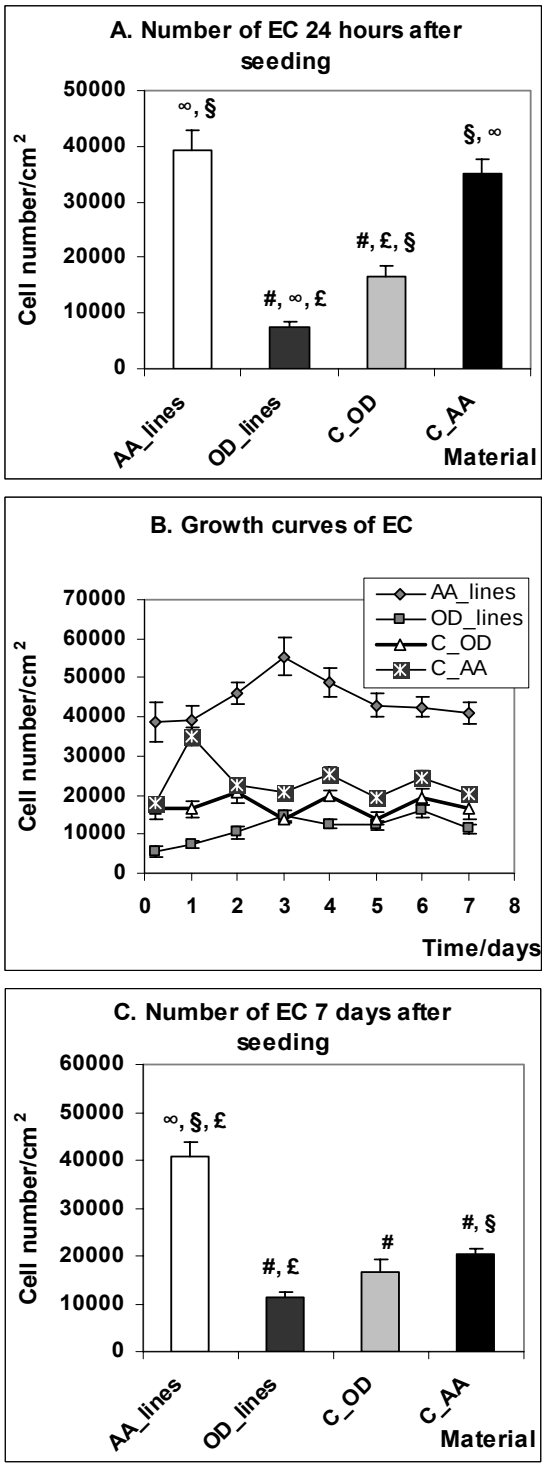
A. Number of EC 24 hours after seeding
Cell number/cm 2
50000
40000
30000
20000
10000
0
∞, §
#, ∞, £
#, £, §
§, ∞
AA_lines
OD_lines
C_OD
C_AA
Material
B. Growth curves of EC
Cell number/cm 2
70000
60000
50000
40000
30000
20000
10000
0
0 1 2 3 4 5 6 7 8
Time/days
AA_lines
OD_lines
C_OD
C_AA
C. Number of EC 7 days after seeding
Cell number/cm 2
60000
50000
40000
30000
20000
10000
0
∞, §, £
#, £
#
#, §
AA_lines
OD_lines
C_OD
C_AA
Material

Fig. 5.

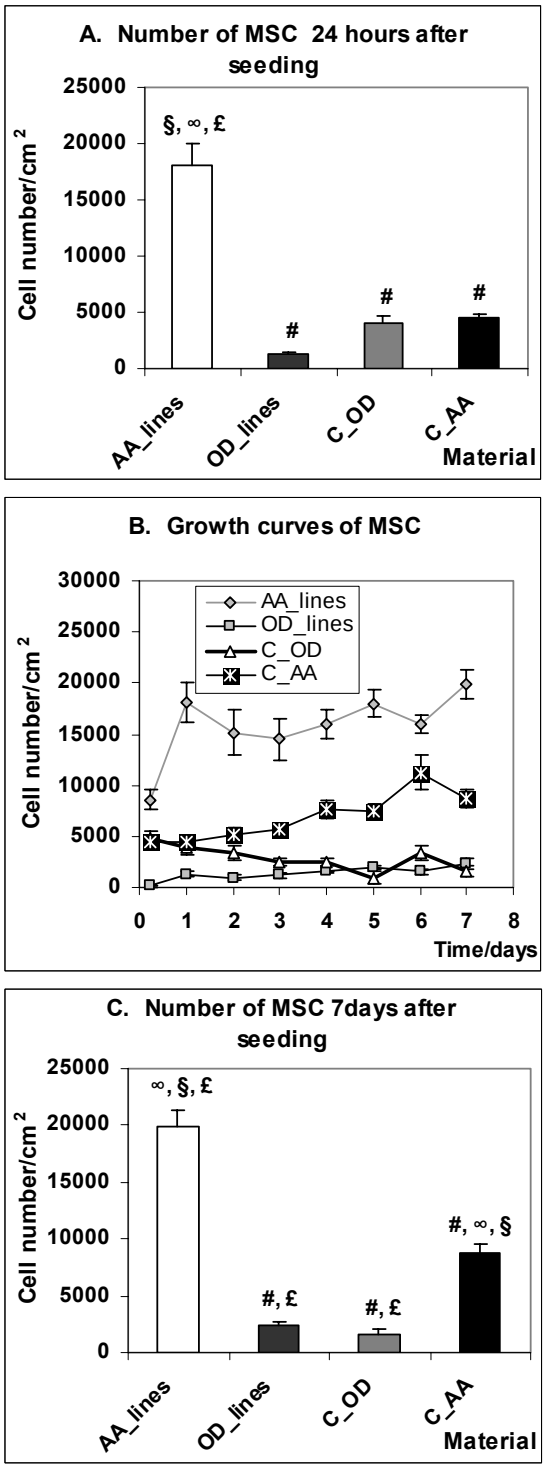
A. Number of MSC 24 hours after seeding
Cell number/cm 2
25000
20000
15000
10000
5000
0
§, ∞, £
#
#
#
AA_lines
OD_lines
C_OD
C_AA
Material
B. Growth curves of MSC
Cell number/cm 2
30000
25000
20000
15000
10000
5000
0
AA_lines
OD_lines
C_OD
C_AA
0 1 2 3 4 5 6 7 8
Time/days
C. Number of MSC 7days after seeding
Cell number/cm 2
25000
20000
15000
10000
5000
0
∞, §, £
#, £
#, £
#, ∞, §
AA_lines
OD_lines
C_OD
C_AA
Material

Fig. 6.

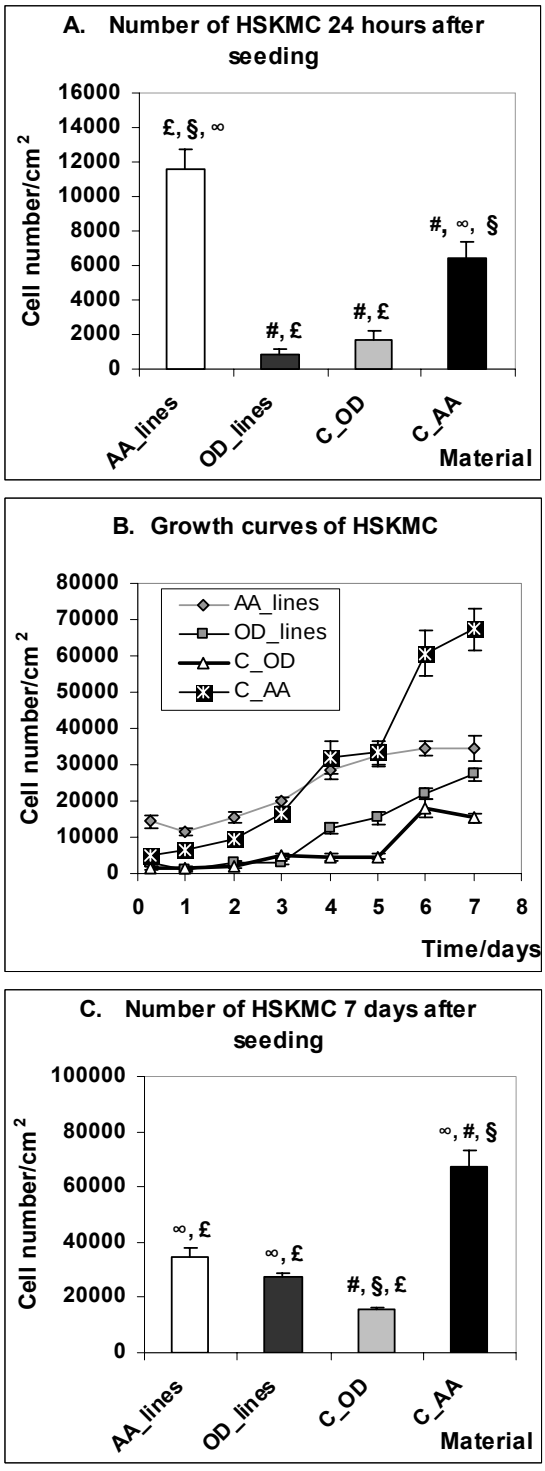
A. Number of HSKMC 24 hours after seeding
Cell number/cm 2
16000
14000
12000
10000
8000
6000
4000
2000
0
£, §, ∞
#, £
#, £
#, ∞, §
AA_lines
OD_lines
C_OD
C_AA
Material
B. Growth curves of HSKMC
Cell number/cm 2
80000
70000
60000
50000
40000
30000
20000
10000
0
AA_lines
OD_lines
C_OD
C_AA
0 1 2 3 4 5 6 7 8
Time/days
C. Number of HSKMC 7 days after seeding
Cell number/cm 2
100000
80000
60000
40000
20000
0
∞, £
∞, £
#, §, £
∞, #, §
AA_lines
OD_lines
C_OD
C_AA
Material

Fig. 7.